LAWRENCE
LIVERMORE
NATIONAL
LABORATORY

LLNL-TR-645057

Final Report --- First principles modeling of microscopic scintillation mechanisms

B. Sadigh

October 21, 2013

Disclaimer

This work performed under the auspices of the U.S. Department of Energy by Lawrence Livermore National Laboratory under Contract DE-AC52-07NA27344.

FINAL REPORT FOR THE PERIOD 2010-2012

PROJECT TITLE: "**First principles modeling of microscopic scintillation mechanisms using a Many-Body Green's function approach"**

webPROJECT NUMBER: LL10-FY10-043-PD05 LAB/CONTRACTOR: LLNL

B&R CODE: DATE: **:** October 15, 2013

LLNL PRINCIPAL INVESTIGATOR: Babak Sadigh, LLNL, (925) 424-6703
LLNL CO-INVESTIGATORS: Daniel Åberg, Paul Erhart, Lorin X. Benedict, Steve Payne

LLNL PROGRAM MANAGER: Jean H. de Pruneda, LLNL, (925) 422-3037

HQ PROJECT MANAGER: Peter Vanier, NA-22, (202) 586-5852

HQ PROGRAM MANAGER: Rhys Williams, NA-22, (202) 586-5001

PROGRESS (BY TASK):

STATEMENT OF WORK TASK LISTING FOR FY 2010:

FY 2010 Tasks:

1. STE and V_k-center formation in NaI and CsI
2. Free carrier lifetimes in NaI and CsI
3. V_k-center migration in NaI and CsI

FY 2011 Tasks:

1. Energy transfer and STE-STE annihilation for NaI and CsI
2. STE interaction with carriers and radiative recombination
3. STE-migration in NaI and CsI

FY 2012 Tasks:

1. Application to $LaBr_3$(Ce)
2. Application to SrI_2(Eu)
3. Application to BaF_2

In 2010, we started the first lifecycle of a project on first principles modeling of microscopic unit processes that occur during scintillation in order to bring about a capability of formulating physics-based reaction-diffusion models that can predict scintillator light yield and explain their non-proportional response to the energy of incident ionizing radiation, with the hope that this will accelerate materials discovery that can mitigate this problem. During the ensuing years we focused on investigating from first principles the elementary quantum mechanical processes leading to polaron formation and exciton self-trapping in scintillators and identify the microscopic pathways leading to their transport.

The effort to derive the master equation for carrier and exciton transport in realistic scintillators materials from first principles constitutes a challenge that requires an extensive background in various areas of computational physics. Previous theoretical investigations involved significant approximations and were limited in their scope. Most notably, the standard workhorse of the computational material scientist, density-functional theory, fails in describing the localized nature of self-trapped carriers as well as the electronic structure of rare-earth dopants. Advances in both algorithms and computational resources however, have rendered a comprehensive and accurate approach feasible. This has been amply demonstrated by the results produced by us during the first lifecycle of this project, which impressed upon the reviewers of the Independent Project Review:

> *"The Review Team agreed, and commented that 'amazing and excellent progress had been made to date.' The researchers tried and did improve the technology to advance the state of the art and show that it was adequate for the project."*

In the following, we detail the progress achieved during each year of the project. We conclude by a final section where all our main achievements are summarized.

FY 2010

Tasks:

1. STE and V_k-center formation in NaI and CsI
2. Free carrier lifetimes in NaI and CsI
3. V_k-center migration in NaI and CsI

We started this project by identifying the computational methodology suitable for quantitative prediction of the electronic structure and thermodynamical properties of V_k-centers. The V_k-center is a localized hole trapped by a particular lattice distortion that in NaI is believed to consist of dimerization of a nearest neighbor iodine pair along the [110]-direction. This is shown in Fig. 1.

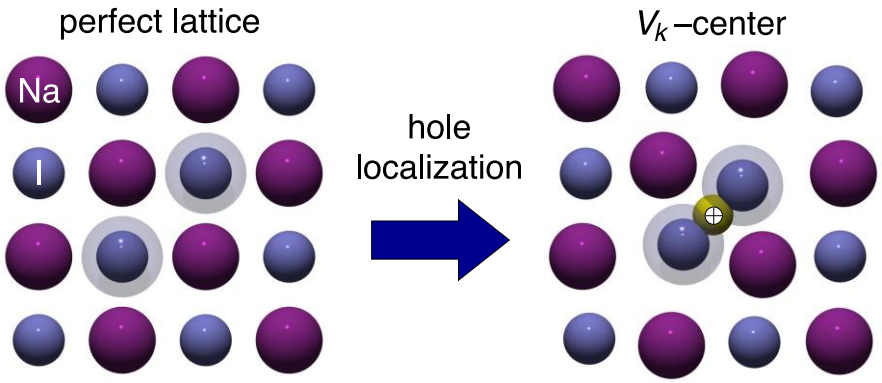

Figure 1: The geometry of a V_k-center, where dimerization of an iodine pair leads to hole localization.

The method of choice for these calculations is a hybrid-sX technique based on an optimal mixture of standard density-functional theory exchange-correlation functional within the gradient-corrected approximation, the so-called PBE-functional, and a screened Fock exchange functional. Determination of system-specific paramerters for the hybrid-sX calculations was a challenge that we tackled in the first quarter of the project. The final parametrization reproduced the band structure, equilibrium density and bulk modulus of the pure crystals in very good agreement with experiment. This allowed us then to conduct a thorough investigation of the electronic structure of the V_k-center in NaI using this methodology.

We thus computed the potential energy landscape of a positively charged NaI crystal (containing a hole) as a function of the separation distance between two neighboring iodine ions, allowing for full lattice relaxation. This is shown in Fig. 2. It illustrates the process of hole trapping through iodine dimerization. At small distortions from the perfect lattice the hole is a delocalized level at the top of the valence band with very weak coupling to the lattice. At about 25% dimerization, a potential energy maximum is reached, which can be identified as the energy barrier (~0.07 eV) between delocalized band-like hole state and the self-trapped state. Beyond this dimerization level, the hole starts localizing and its eigenenergy separates from the top of the valence band and moves inside the gap (see Fig. 2b).

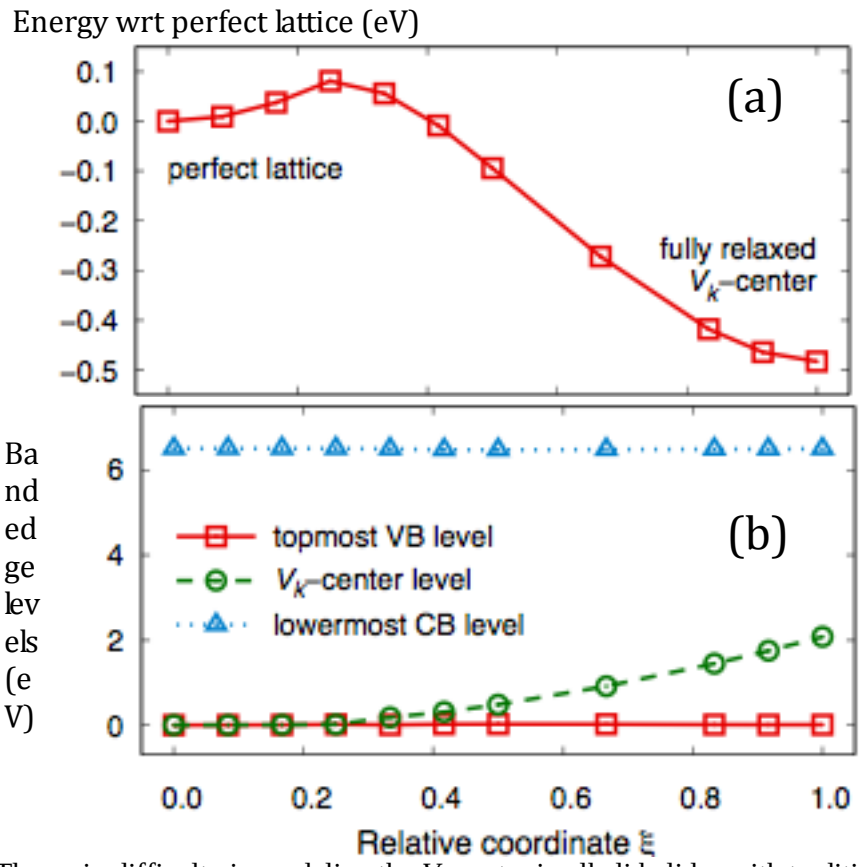

Figure 2: Hole energy in NaI relative to the perfect lattice configuration (a), and the single-particle levels (b), for fully relaxed configurations containing an iodine pair with different levels of dimerization, where ξ=0 corresponds to the perfect lattice and ξ=1.0 corresponds to the V_k-center.

The main difficulty in modeling the V_k-center in alkali halides with traditional electronic structure techniques has been to localize the hole charge density in the presence of lattice distortion. To further showcase the validity of our approach, we visualize in Fig. 3 below the changes in the charge density of the V_k-center along the transition from the perfect lattice to the final self-trapped configuration. It shows the completely delocalized hole charge in the perfect lattice and fully localized one in the self-trapped case. Note the incipient localization taking place in the hole charge density of the saddle point configuration.

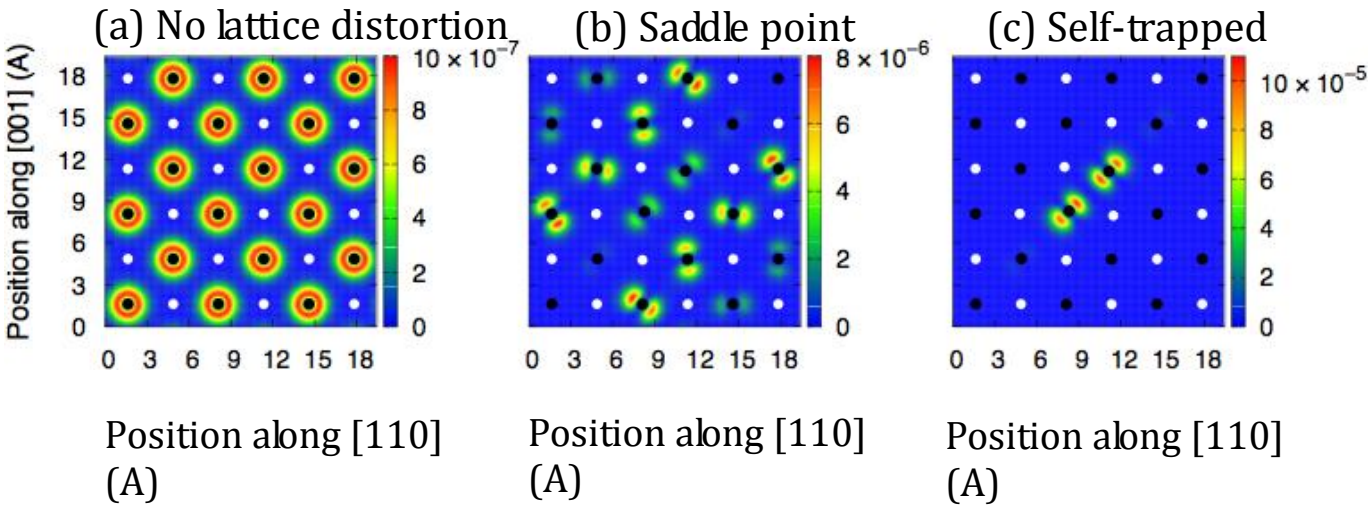

Figure 3: Hole charge density distribution in NaI crystal for three configurations along the self-trapping path.

In summary, we find that the fully relaxed V_k-center configuration the two iodine ions, at which the hole is localized are 3.24 A apart, to be compared with a separation of 4.58 A in the perfect lattice and a separation of 2.67(3.3) A in the netural I_2 (singly charged I_2^-) molecule. The V_k-center in NaI is thus very similar in character to an I_2^- molecule embedded in a matrix. The binding energy of the localized hole to the trapping iodine dimer is ~0.4 eV.

For the purpose of organizing our results towards original publications of significance in the field of fundamental physical modeling of scintillator materials, we went ahead and applied our previously successful methodology in calculating the formation energy of the V_k-center in NaI to all alkali halides. This is shown in Fig. 4 below, where the formation energies of alkali-fluorides, chlorides, bromides and iodides are all collected in one graph. We had originally found that NaI has an STH formation energy of about 0.4 eV, which seemed quite large. However, studying this quantity in genral we find that the iodides have the least bound STH defects. In fact the formation energy of a V_k-center in LiF can be as large as 1.6 eV. This is a huge energy imparted to the lattice whenever a self-trapped hole is formed and can explain observed radation-induced defect formation in these systems. The major trend found is that the STH formation energy is highly correlated to the band gap, in turn determined by the halogen type of the compound. In the left panel of Fig. 4 it is shown that the formation energy is uncorrelated to structural parameters such as the Rabin-Klick parameter. This is in contrast to most other physical properties of these systems, such as Stokes shift, where Rabin-Klick parameter is the main order parameter.

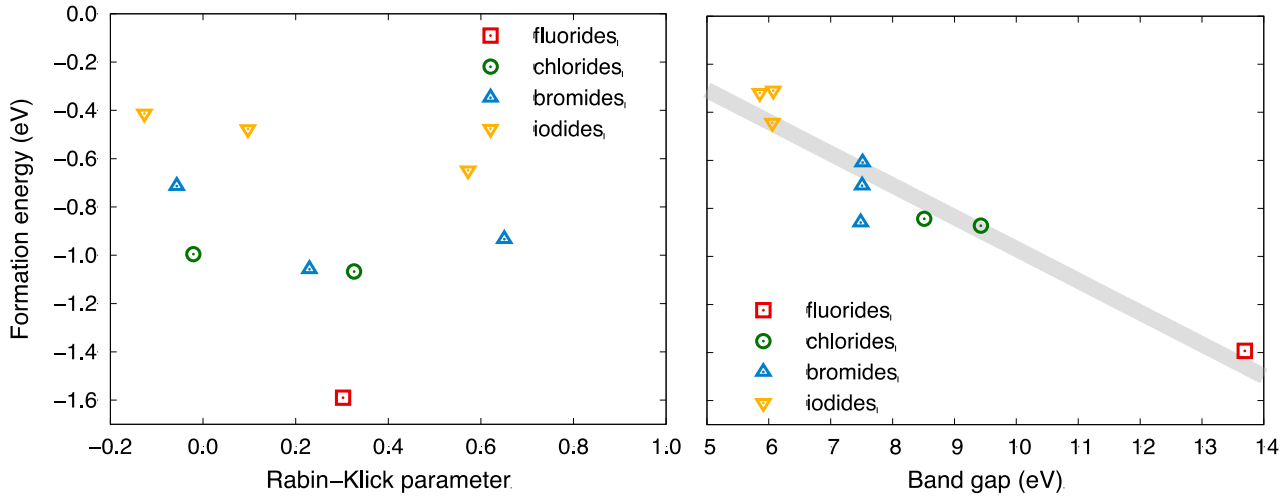

Figure 4. The formation energies of V_k-centers in all alkali halides with rock-salt crystal structure. The different compounds are colored depending on the halogen ion. Note the large variation in the formation energies from 0.2 to 1.6 eV. The left panel depicts the formation energies as a function of the ubiquitous Rabin-Klick geometric parameter. The right panel shows the same dependence as a function of the material band gap. From the right panel we conclude that the band gap of the compound is a good predictor for the energetics of the formation of self-trapped holes.

Once we had managed to fully explore the geometry and energetics of V_k-centers, we embarked on the hybrid+sX calculations for obtaining stable self-trapped exciton (STE) configurations in NaI. The problem of stable STE configurations in NaI was found to be a more difficult task with delocalized electrons and multitude of low-energy configurations, so-called on-center and off-center configurations. In the figure below we illustrate the charge density distribution of the electron and the hole components of the STE in NaI. It is shown the hole component is highly localized around the iodine dimer while the electron component is relatively diffuse with large spread.

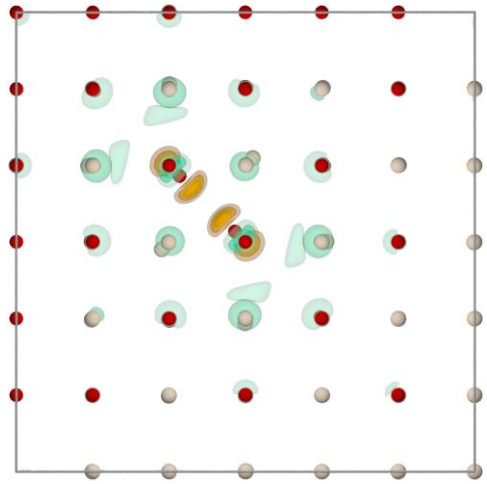

Figure 5. The charge density distribution of the hole (orange) and the electron (green) components of the STE in NaI.

The Stokes shift is the difference in the absorbed and the emitted photon energies in optical measurements. The reduction in the energy of the emitted photons relative to the absorbed photons is due to lattice coupling. It can be described as the lattice relaxation in the presence of an exciton. The variety of the obserbed Stokes shifts in experiments have provided for deep conclusions to be drawn concerning the structural and magnetic properties of STEs in alkali halides. In principle alkali halides can be classified into different groups depending on the multitude of the Stokes shifts they exhibit. In short, the observations of Stokes shifts have lead to the understanding that beside the spin-singlet and triplet states of excitons, they also can appear in on-center and various off-center ionic configurations. We have in particular studied these issues in detail during the past quarter for NaI. The energies of the ground state as well as the excited state electronic structures as a function of on-center and off-center relaxation coordinates are shown below for the two hybrid functionals PBE0 (left panel) and m-HSE06 (right panel).

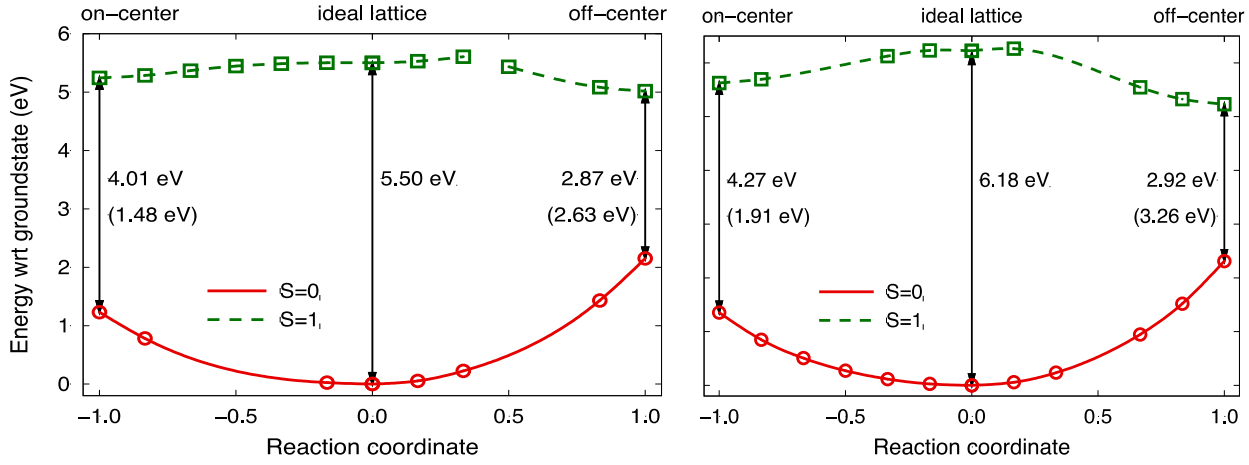

Figure 6. Potential Energy landscape of the exciton in NaI as a function of reaction coordinate towards on-center as well as off-center STE geometry. The left panel shows the energetics calculated from PBE0 functional and the right panel shows that of the modified HSE06. The red curves correspond to spin-singlet ground state, while the green curves show the spin-triplet state energies. The numbers in parantheses are the calculated Stokes shift, that should be compared with the experimental value of 1.1 eV.

The experimental Stokes shift for this system is found to be 1.1 eV and is interpreted to be originating from the on-center configuration. As shown in the above figure, the PBE0 prediction for the on-center Stoke-shift is 1.48 eV

while the m-HSE06 functional yields the value 1.91 eV. We have devised an original method based on GW technique that can correct the error in the Stokes shift from the hybrid functional. Using this technique we obtain a value of 1.27 (PBE0+G_0W_0) and 1.40 (m-HSE06+ G_0W_0) for the on-center Stokes shift in much better agreement with experiments. One important discrepancy of the hybrid method is that the NaI-off-center configuration with a Stokes shift of 2.63 eV (PBE0), 3.26 eV(m-HSE06) is in fact lower in total energy than the on-center configuration in stark disagreement with experiments.

FY 2011 Tasks:

1. Energy transfer and STE-STE annihilation for NaI and CsI
2. STE interaction with carriers and radiative recombination
3. STE-migration in NaI and CsI

Once the equilibrium geometry and thermodynamic properties of the self-trapped hole in NaI was established, we went ahead with calculating a much more complex quantity, namely the transport/migration of this specie. We thus identified four fundamental high-symmetry atomistic pathways and associated energy barriers for V_k-center migration. These are:

(i) rotation through 60° from [110] to [101],
(ii) rotation through 90° from [110] to [1-10],
(iii) rotation through 180° or translation along [110],
(iv) rotation through 120° from [110] to [101].

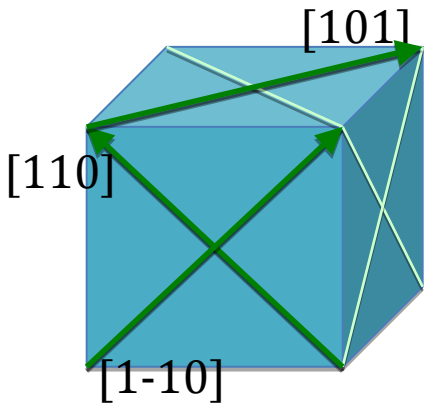

The rotation mechanism iv, had never been proposed in the past, and was first conceived by us. We found that in agreement with experiments the migration pathways involving 60° rotations of the V_k-center have the lowest energy barrier and thus are the most probable. However, we found that the calculated energy barrier (0.25 eV) is somewhat larger than experiments (0.18 eV). This is most likely due to the deficiencies of the hybrid-sX approximation to the electronic exchange and correlation.

One of the very important achievements of our project came next when we calculated the migration barrier of the STE following the same mechanisms explored for the V_k-center as described above. In the past it had always assumed that the STE diffuses through the lattice much faster than then self-trapped hole. However, our finding that the electron component of the STE in NaI is quite weakly bound and thus delocalized suggested to us that the STE migration barrier should mainly be dictated by the hole component. This conjecture was confirmed by us, through painstaking calculations of the four transition pathways described above applied to supercells containing an STE. We thus found out that the STE in NaI is as immobile as the V_k-center, with a migration barrier of about 0.25 eV.

This information was communicated to the PNNL group, whereupon they modified their kinetic Monte Carlo transport models.

As the STE is quite a complex specie, its motion through the lattice can lead to a manifold of events, such as defect production and annihilation. We thus spent a large effort on studying the coupling of STEs to the lattice in order to make predictions on the STE motion leading to defect production as well as phonon-assisted annihilation. Figure 7 below shows the potential energy landscape for the STE in NaI. The configuration at the origin of Fig. 7 is the on-center NaI-STE configuration, which in agreement with experiment is the lowest energy configuration. The figure illustrates the STE potential energy along three different pathways from the stable on-center configuration to a one-step separation of a vacancy + interstitial complex, so-called F+H pair.

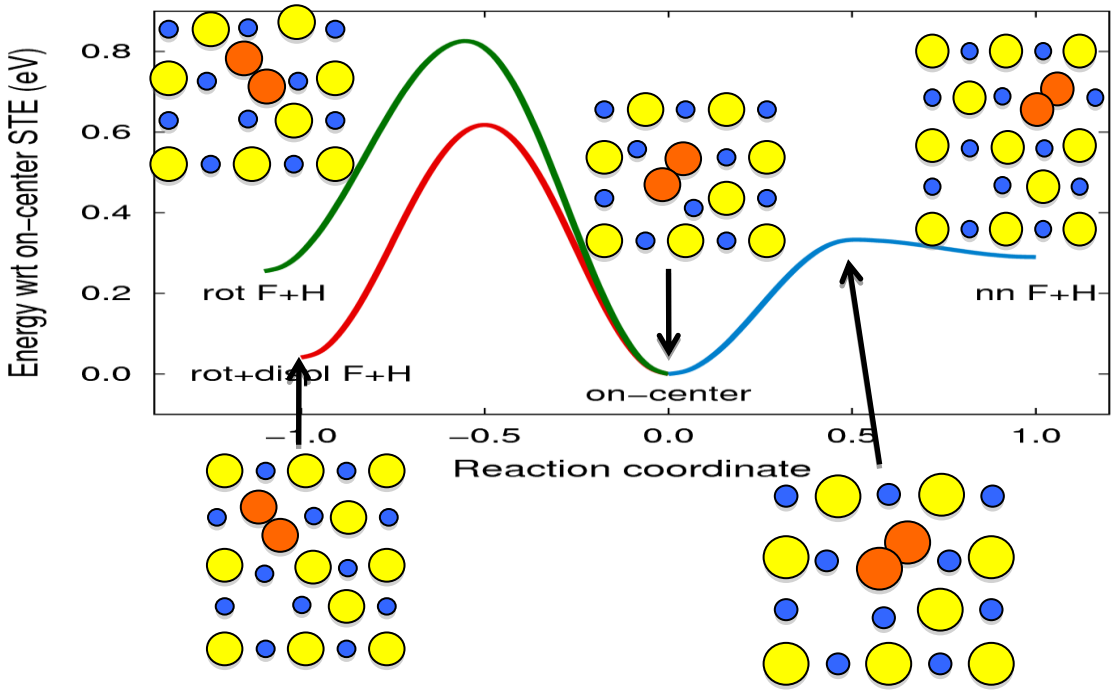

Figure 7. Potential Energy landscape of the self-trapped exciton in NaI. The curves with different colors (blue/red/green) represent reaction coordinates along three different pathways starting from the on-center configuration to partial separation, i.e. nearest-neughbor F+H configurations. In particular, the transitions represented by the red and green curves lead to annihilation. To clarify the geometry, a few STE structures along the transition pathways are explicily depicted.

The significance of the above potential energy landscape is in describing the movement of an STE mainly with respect to its dissociation into a vacancy and an interstitial. The energy difference between the configuration at the coordinate 1.0 (nn F+H) and the one at the origin (on-center) is the barrier to STE dissociation.

In the above figure the rotated+displaced F+H pair configuration does seemingly have lower energy than the on-center STE configuration. The explanation for this is shown in Fig. 4 below, where the topmost valence band and the bottommost conduction band states as a function of reaction coordinate (along the path to rot+displ F+H corresponding to negative coordinates in Fig. 3) are shown. It is seen that the band gap collapses along this pathway, whereupon the conduction band and the valence band cross at the saddle point located at -0.5 in Fig. 3 above. This is significant result showing a possible phonon-assisted STE annihilation mechanism.

An important milestone that was completed in the second year was the many-body calculation of the excitonic contribution to the dielectric function of NaI and more importantly for our project free exciton binding energy in this system. The dielectric function was already calculated in FY2010. However, the total energy of the exciton still remained a challenge since it requires much more computations. In fact this quantity can only be converged by linear asymptotic extrapolation of a set of calculations with varying number of k-points sampled in the Brillouin zone. This is shown in Fig. 8 below. The fee exciton binding energy of ~0.22 eV is an important parameter that

determines the ratio of "born excitons" after the initial carrier thermalization period of ~1fs. The really interesting physics now would be emerging once the self-trapped exciton versus the free exciton properties of systems such as SrI_2 and $LaBr_3$ were to be calculated and compared. This would let us understand the correlation of these quantities with non-proportional response of these systems. Hence, we were ready to embark on our final endavour in this project, i.e. the unknown polaronic/excitonic properties of a complex system such as SrI_2.

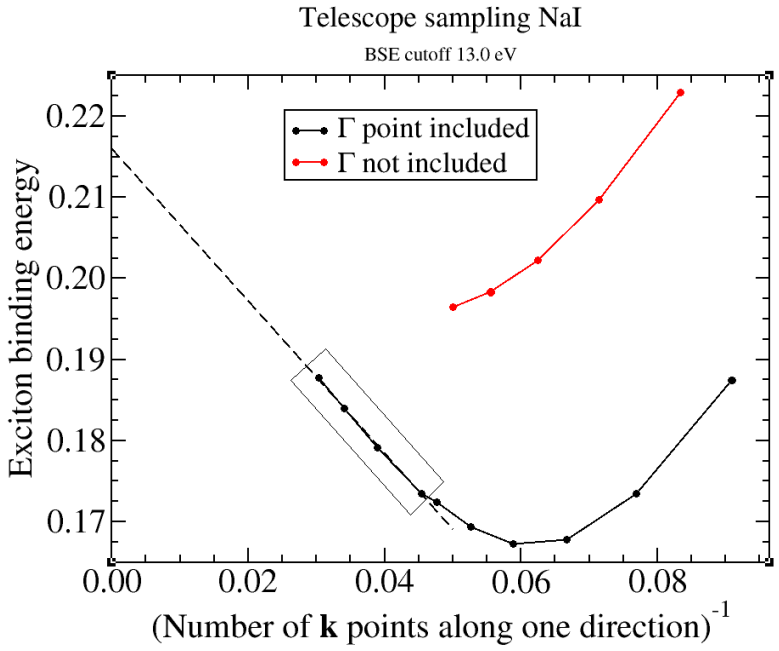

Figure 8. Calculation of the binding energy of the exciton in NaI by extrapolating from a set of calculations with finite k-point sampling.

FY 2012 Tasks:

1. Application to $LaBr_3$(Ce)
2. Application to SrI_2(Eu)
3. Application to BaF_2

Once the hybrid-DFT methodology proved successful for the polarons and excitons in alkali halides, we embarked on the unprecedented study of the structure and energetics of self-trapped holes and excitons in SrI_2. The caveat here is that the crystal structure is complex and no apriori knowledge of the structure of even STHs exist. Hence any predictions on their atomistic/electronic nature constitutes completely original contribution to the field where no one has ever gone before. Figure 9 below, shows one unit cell of the crystal structure of SrI_2. It contains 24 atoms with two inequivalent iodine sites. The anisotropy of this structure manifests itself in strongly anisotropic elasticity, which is both measured experimentally and reproduced in our calculations.

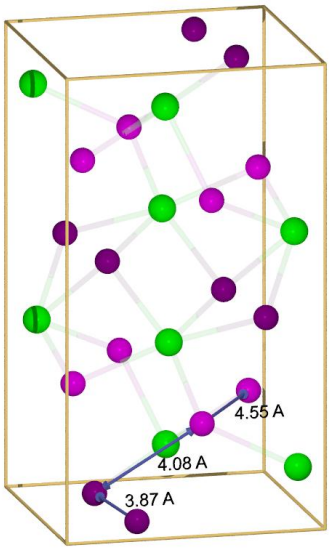

Figure 9. The perfect SrI_2 crystal structure. The unit cell contains 24 atoms. Two inequivalent iodine sites exist with three different nearest-neighbor iodine pair distances (4.55 A, 4.08 A, 3.87 A) as shown in the Figure. This structure is highly anisotropic, which is confirmed by our first-principles calculations for the elastic constants of this material.

We commenced by first focusing on investigating the ground state electronic structure of SrI_2. At the start of our effort, there were only scarce experimental information concerning the band structure of this material in general and its band gap in particular. Since density-functional theory does severely underestimate band gaps, and hybrid-DFT is not a parameter-free approach, we could only resort to many-body perturbation theory calculations within the GW scheme. In this way, we obtained our first success, that of calculating the band structure of SrI_2 with GW and predicting its band gap to be 5.5 eV. Subsequent experiments confirmed our calculations.

Next, we focused our attention on finding low-energy self-trapped hole configurations in SrI_2. Due to the high complexity of the SrI_2 crystal structure, it is not computationally expedient to explore the geometry of the self-trapped hole entirely via the hybrid technique. While the latter is expected to give quantitative prediction of the energetics/structure of the self-trapped hole, we resorted to the strategy to construct a simpler and cruder model that can qualitatively capture the electronic structure of SrI_2. We can then use this simpler model to make a few initial guesses for reasonable STH configurations, which we then refine by quantitatively exploring the nearby potential energy landscape via the hybrid-DFT technique.

In practice, we used the LDA+U formalism for the crude model, and we have performed ab-initio molecular-dynamics (MD) to simulate the kinetics of hole self-trapping as described by thus-parameterized LDA+U model in order to provide initial guesses for the configuration of the self-trapped hole in SrI_2. In particular for SrI_2, we found that the electronic structure (most importantly) in the proximity of the band gap can be reasonably described by PBE-parametrization of Generalized Gradient Approximation plus U=10 eV. MD simulations SrI_2 + one hole, using this LDA+U parametrization was shown that this model allows for hole self-trapping to occur in this system. The localization of a hole is easy to verify in electronic structure calculations, since it leads to spin polarization. Hence following the spin density in MD simulations, one can track the kinetics of hole localization and migration.

We have identified several distinct STH configurations generated by the MD simulations described above. These configurations have been further studied quantitatively using the hybrid PBE+sX technique. In this way we have found three possible STH configurations in SrI_2, as shown in Fig. 10 below. These configurations are bound by 0.17 eV, 0.03 eV, and 0.23 eV respectively, relative to the undistorted crystal plus a delocalized hole. The lowest energy configuration (see Fig. 2-(c)) is bound by 0.23 eV, which is very close to the V_k-center binding energy in NaI.

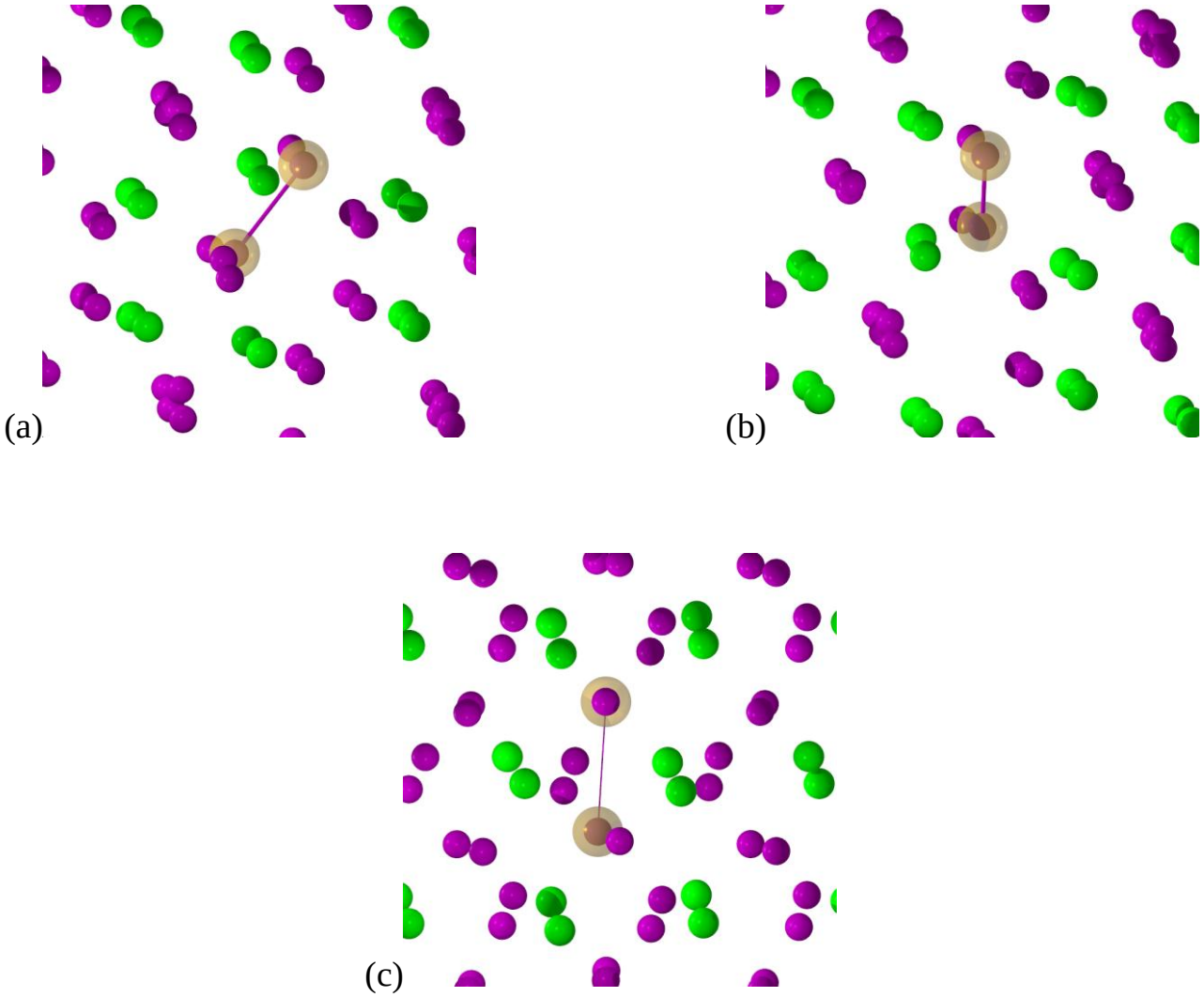

Figure 10. Three self-trapped hole configurations in SrI_2 has been discovered. The purple spheres represent I atoms and the green are Sr atoms. (a) STH is bound by 0.17 eV, with an iodine pair originally at 4.09 A collapsing to 3.32 A. (b) STH is bound by 0.03 eV, with an iodine pair originally at 4.55 eV collapsing to 3.32 A. (c) STH is bound by 0.22 eV, with an iodine pair originally at 3.87 A which only reduces its bond length to 3.6 A.

The self-trapped hole configurations shown above are remarkable in one important aspect. It is quite well-known that in nearly all alkali/alkaline-earth halides the STH configurations consist of negatively charged halogen dimers with the dimer distance very similar to that of the free radical. The two high-energy STH configurations (a) and (b) in Fig. 2 above do follow this trend and contain I_2-dimers at a distance of 3.32 A. However, the lowest energy STH (c) configuration above corresponds to an iodine pair with a bond length of 3.6 A. This is in stark contrast with almost all known STH configurations, and has important consequences for the hole migration as well as STE formation/migration in this system.

Next we explored the possibility of polaron formation of electron carriers in SrI_2. This was inspired by the observation of significant electron binding in the STEs derived from STH configurations capturing an electron. This finding was in stark contrast to our previous experience with NaI where the electron component of the STE is quite delocalized. This result can be understood in terms of the characters of the conduction bands of the of SrI_2 and NaI. Whereas the former consists mainly of Sr-derived *d*-electrons, the latter has *s*-type character.
By the end of the 1st quarter of 2012, we were thus suspecting that self-trapped electrons (STe^-) may exist in SrI_2, and during the second quarter we finalized our search into the nature of these species. Our main result has been the identification of self-trapped electron configurations corresponding to Sr-Sr dimerization, where the bond length in perfect crystal of 4.7Å collapses to 4.3Å around the self-trapped electron. Figure 11, below shows the localization that occurs due to self-trapping. Note the d-symmetry of the charge distribution of this polaron. This kind of

localization was never observed in the case of NaI. For that system, not only stable self-trapped electrons do not form, but the electron component of the STE is quite delocalized. This is expected since the conduction band in NaI consists of Na s-states.

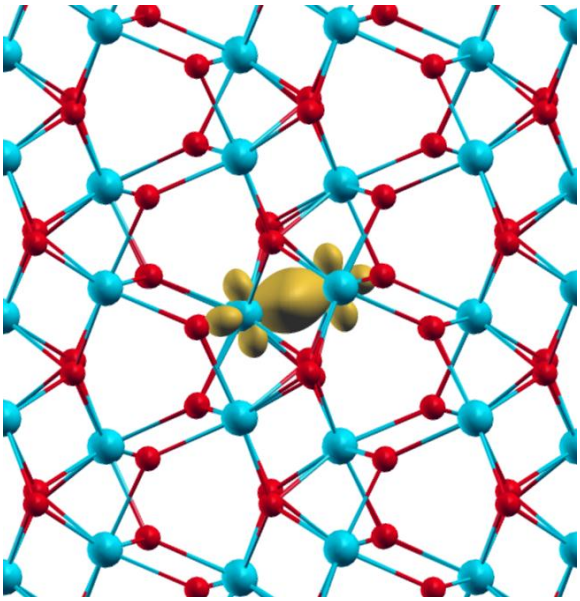

Figure 11. The charge distribution of the self-

In summary, we have found two distinct lattice distortions, one involving Sr-Sr dimerization that corresponds to electron polarons and one involving I-I dimerization, which corresponds to hole polarons. Since we are the first to have identified the geometries of polarons in SrI_2, we have also been in excellent position to explore whether they lead to a multitude of STE configurations. As expected we find two classes of STE configurations: (i) those derived from STe^- and those derived from the STH. The two kinds of STEs are very close in energy. The STH-derived one is the lowest in energy by less than 20 meV. We have further investigated the electronic structure of all the polarons and STEs in SrI_2. The electronic levels introduced in the bandgap are summarized in Fig. 12 below. Note that we calculate luminescence energies for the STEs in SrI_2 to be between 4.2-4.38 eV.

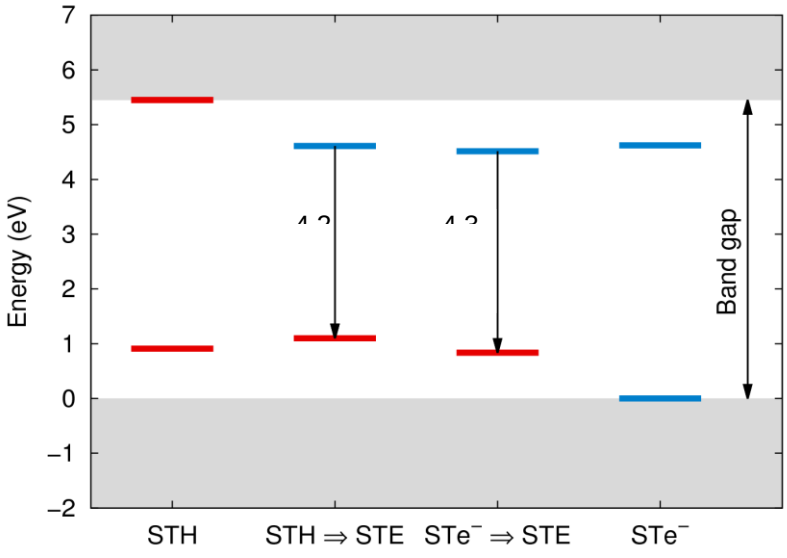

Figure 12. The electronic levels inside the band gap for several polaron and related self-trapped exciton configurations.

With the polarons and STEs in SrI_2 having been exhaustively studied within hybrid-DFT approach, we embarked on our final deliverable, i.e. the free exciton distribution and binding energy in this system using many-body perturbation theory leading to the BSE approach. As was explained above, the binding energy of an exciton is numerically a very demanding quantity to calculate. The calculations converge only asymptotically for extended (Wannier-like) excitons since the long-range Coloumb kernel causes very slow convergence of the reciprocal space

integrals over the first Brillouin zone. This presented us with quite a hurdle for calculating exciton binding energies in SrI_2, since performing k-point convergence for the already complex chemistry of this material requiring a 24-atom supercell, could become computationally prohibitive. While we had managed to perform binding energy calculations for NaI via k-point asymptotics, it was not clear to us how difficult it would be to obtain numerically significant results for SrI_2. This is work at the absolute forefront of research in this field. Figure 13 shows the exciton binding energy calculations in SrI_2 as a function of the density k-point sampling of the Brillouin zone. Due to the complexity and anisotropy of the crystal structure, k-point density could be varied in different ways along the differet axes of the unit cell.

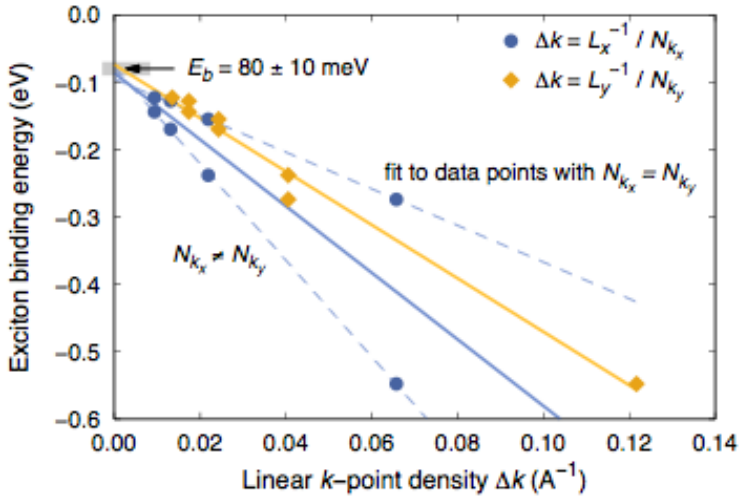

Figure 13. Calculation of the binding energy of the exciton in SrI_2 by extrapolating from a set of calculations with finite k-point sampling. By extrapolation a binding energy of 0.08 eV is obtained.

Linear extrapolation in Fig.1 leads to a free exciton binding energy of 0.08 eV to be compared with that of 0.22 eV in NaI. This is by itself a very surprising result. Since SrI_2 is one of the brightest and most proportional scintillators one might have expected for excitons in this system to be strongly bound. However, our results suggest that the excitons are much more bound in NaI than in SrI_2. One may wonder how this then reconciles with the empirical knowledge that SrI_2 is so bright and proportional. The conclusion is that the carrier transport away from the track must be efficient in this system and that annihilation rates must be low. We have above reported on our extensive studies concerning self-trapped carriers in SrI_2, where we found that both electrons and holes self-trap in SrI_2 with moderate binding energies, while in NaI holes bind very strongly to lattice distortions (self-trapped holes are practically immobile) and electrons are delocalized band carriers. We can reasonably argue that the total carrier transport is determined by the slowest carrier and in this way it becomes clear that effctive mobility is higher in SrI_2 than in NaI. Of course, calculating annihilation and diffusion rates quatitatively is part of our future goals in this project.

An unexpected result regarding the electron/hole distribution of the lowest-energy exciton was found in the BSE calculations with perhaps important consequences. The effective hole distribution for this exciton is shown in Fig.14 below. Note the layered structure, which indicates that each such exciton is localized within a plane. Hence we anticipate the lowest-energy excitons to exhibit two-dimensional transport. This anisotropy in exciton mobility in SrI_2 is similar to the anisotropy observed in the elastic constants of this system.

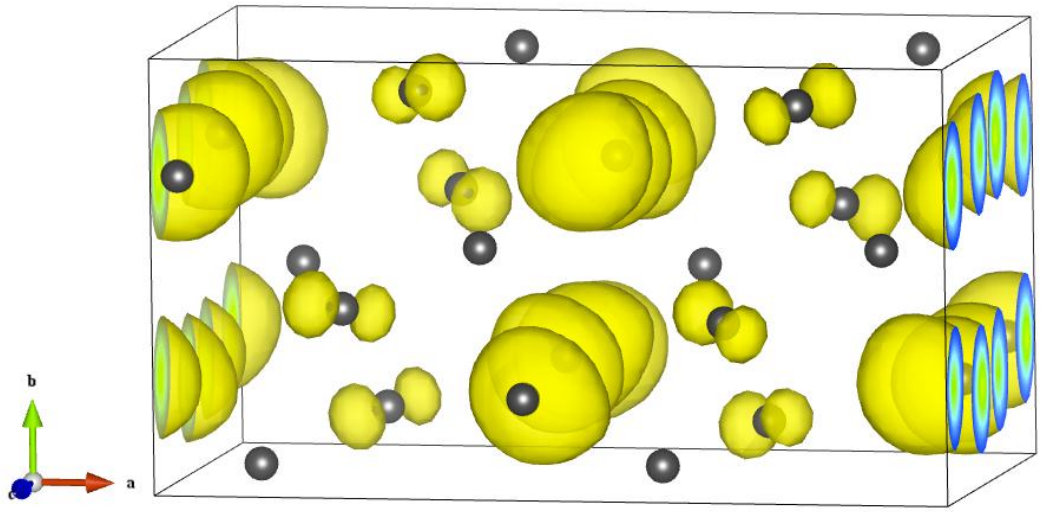

Figure 14. The distribution of the hole-component of the lowest-energy exciton in SrI_2.Note the layered structure with small overlap between the layers, which is a signature of localization of the exciton inside each plane.

We also performed considerable work on the electronic structure and excitonic properties of $LaBr_3$. This system constitutes a particularly challenging case, due to spin-orbit coupling and subtle interactions between the 5*d* and the 4*f* states, which cannot be reproduced by standard density-functional theory approaches. We performed a detailed investigation of the electronic structure of $LaBr_3$ using the quasiparticle self-consistent GW (QSGW) method. We identified the effect of spin-orbit coupling in splitting La-derived states, in particular La-4*p*, as well as the role of inclusion of correlation effects in determining the position of the La *f*-level in the conduction band. We have been able to explain some of the features observed in the measured absorption spectra of this system in terms of the densities-of-states of the *d*- and the *f*-bands as calculated within the QSGW technique. We also use the QSGW results to benchmark several computationally less demanding techniques such as LDA+U, hybrid exchange-correlation functionals as well as G_0W_0. Figure 15 summarizes all these results by juxtaposing the densities-of-states from all the computational techniques used in this work.

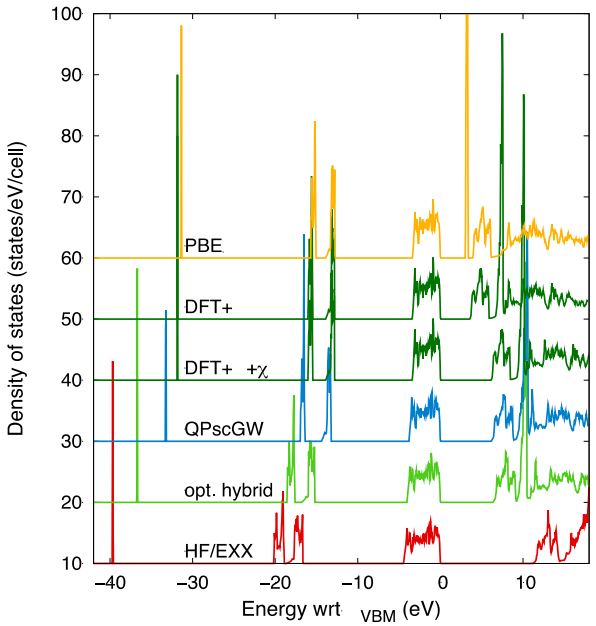

Figure 15. Densities-of-states as obtained from various approximations to exchange and correlation in $LaBr_3$.

With regards to excitonic properties in $LaBr_3$, we have calculated the dielectric function and optical absorption spectra of this system explicitly including two-particle (electron-hole) correlations through solving the BSE. Below, we illustrate our calculated electron-hole pair-correlation function from the solution of the BSE equations in $LaBr_3$.

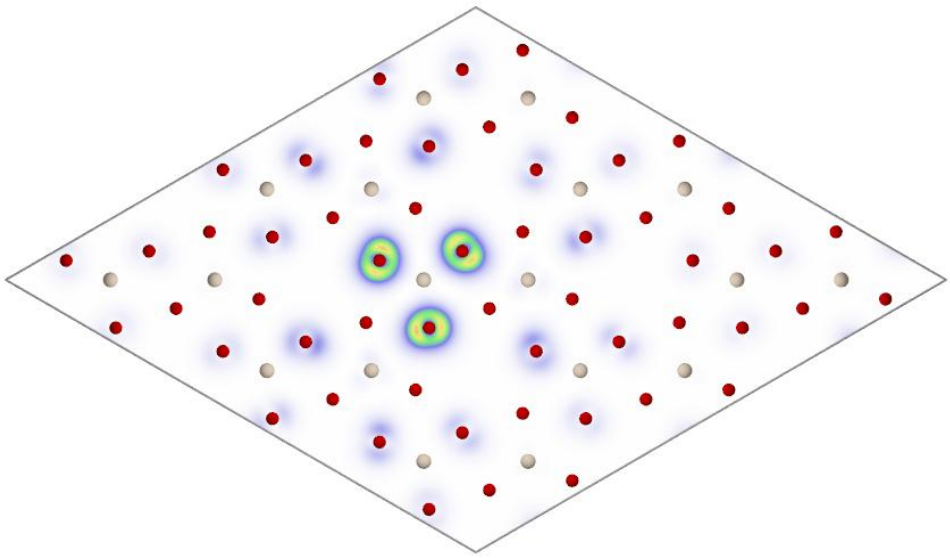

Figure 16. Distribution of the hole component of the lowest energy exciton in $LaBr_3$, around an electron centered on a La atom.

Summary of achievements

During the first lifecycle, we have in great detail studied the self-trapping mechanisms of holes and excitons in alkali halides (AHs) as well as SrI_2 from first principles electronic structure theory. For this purpose, we have explored the hybrid DFT+screened exchange, the GW technique as a non-self-consistent perturbation theory, the self-consistent quasiparticle GW method, and finally the highly computationally demanding Bethe-Salpeter-Equation (BSE) approach that explicitly includes excitonic effects. We have successfully reproduced the known experimental geometries for the simple AHs and have *calculated quantities that were previously unknown*, such as the significant local heating due to energy release that occurs when a hole is self-trapped in AHs. However, as mentioned above, one of the most important goals of the first lifecycle has been to obtain quantitative understanding of the microscopic processes behind carrier and exciton transport in realistic scintillator materials during the low-energy transport (LET) stage after the initial ionization spanning the time scale from one femto-second to several nano-seconds. For this purpose, we have focused on the classic scintillator material NaI, and have calculated the mechanisms and rates of diffusion of STHs and STEs in this system. Subsequently, in collaboration with the PNNL group we have derived the basic dynamic equations governing the evolution of carrier and exciton distributions during the LET stage. This collaboration has constituted one of the cornerstones of our project. The choice of NaI has been partly motivated by the importance of this system as scintillator material while having fairly simple crystal structure, but also due to the fact that a wealth of experiments, done over several decades, are available that may be used to validate our approach. Nevertheless, we have made several discoveries that significantly modify the current understanding of the carrier/exciton transport during the LET stage. In this regard, our most important contribution has been through calculations of STE migration that has shown their diffusivity to be very similar to STH, contrary to the conventional expectation in the field that the former diffuses much faster than the latter. This has qualitatively changed the picture of the dynamical evolution STEs and STHs prior to reaching the activators in this system.

From the standpoint of scintillator physics, our most significant achievements have been the prediction of energies and geometries associated with self-trapping of holes, electrons and excitons in the complex crystal structure of SrI_2, where no information on the structure and multiplicity of either STHs or STEs exist in the literature. In particular with regards to self-trapped electrons (STe^-), there has not even been an expectation of their formation in the literature. In short, we have found two

distinct lattice distortions, one involving Sr-Sr dimerization that corresponds to electron polarons and one involving I-I dimerization, which corresponds to hole polarons. Since we are the first to have identified the geometries of polarons in SrI_2, we have been in excellent position to also explore whether they lead to a multitude of STE configurations. By now, we have found two classes of STE configurations: (i) those derived from STe^- and those derived from the STH. The two kinds of STEs are very close in energy. As a result, a surprisingly rough potential energy landscape underlying STE migration emerges, which contains a multitude of shallow minima that can facilitate relatively rapid migration for this specie.

Our discoveries point to stark differences between SrI_2 and NaI with regards to charge and exciton localization in these systems. This can go a long way to explaining the observed differences in non-proportionality in these two systems. In particular, we have found that the electrons and the holes in SrI_2 are similarly localized, with similar mobilities. This finding is in stark contrast to our previous experience with NaI where the electron component of the STE has shown to be quite delocalized. This result can be understood in terms of the characters of the conduction bands of the of SrI_2 and NaI. Whereas the former consists mainly of Sr-derived *d*-electrons, the latter has *s*-type character. The delocalized electrons in NaI are orders of magnitude more mobile than the V_k-centers, and lead to high STE-STE annihilation rates. Based on these facts, it is reasonable to expect that undoped NaI has very low light yield, in agreement with observations. Our comprehensive charaterization of the polarons and STE in SrI_2 in conjunction with recent experiments at WFU are bringing about a very interesting picture that can help explain the unusual high light yield and proportionality in this system. These findings can provide guidelines for designing scintillator materials with optimal resolution.

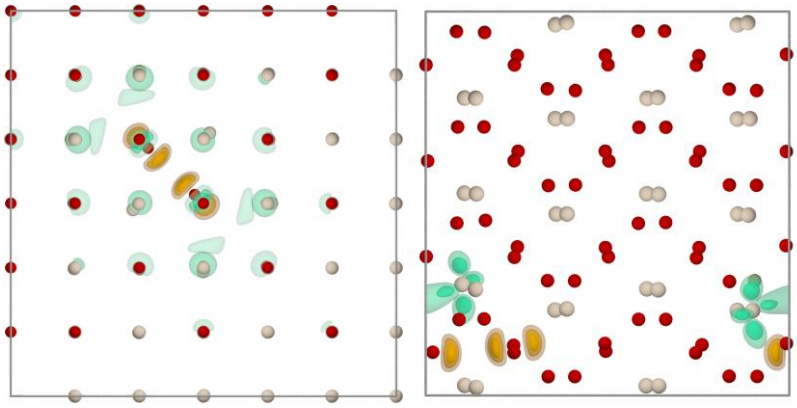

Electron (cyan) and hole (orange) densities for triplet excitons in NaI (left) and SrI_2 (right). Note that while the hole and the electron distributions in SrI_2 are similarly localized, the electron in NaI is much less localized than the hole. Iodine atoms are colored red, whereas the anions are white.

Another important achievement of the first lifecycle that will play an important role for our future work in this area has been the successful application of the complex BSE machinary to solving the problem of explicit electron-hole Coloumb interaction leading to excitonic binding. This is in particular important for describing free exciton formation energy and annihilation rates. These calculations are computationally very demanding, but by now we have not only succeeded in performing calculations for NaI, but we are currently also concluding computations of the excitonic effects in SrI_2. The free exciton binding energy is an important parameter that determines the ratio of "born excitons" after the initial carrier thermalization period of ~1fs. This provides the necessary initial condition for the reaction-diffusion equations in the LET stage.

In terms of method development we have implemented novel features that allow for efficient calculations when the relativistic spin-orbit (SO) interaction is important, which is the case for scintillator materials with high stopping power. This has led to an order-of-magnitude decrease in computational cost and for the first time made relativistic GW calculations for SrI_2 and $LaBr_3$ tractable. Along the same lines, we have made and are continuing several important methodological developments that allow us to perform unprecedented calculations of the geometries and band structures of both singlet and triplet self-trapped excitons. With inclusion of SO coupling, we are now at a point where we can calculate Auger annihilation, as well as radiative recombination rates of excitons. Coupled with our new ideas for better scaling with respect to supercell size we are well equipped to lead the field in this area. These algorithmic developments will be also of interest to modeling the electronic structure of complex semiconductors.

Discussion of any anticipated funding shortfalls: None

Identify any LDRD that may be relevant to improving this project: None

COSTING: We have been spending at a rate of $25K/month. The spending is on target.

TECHNICAL REPORTS/PUBLICATIONS (BY TASK):

PNNL/LBNL/LLNL Workshop on Scintillator Physics was hosted by LLNL on December 18, 2009201. Oral presentation entitled "First principles modeling of microscopic scintillation mechanisms**".** This title is implied below unless explicitly specified.

Poster was presented at the Radsensing2010 meeting (June 8-10) at ANL.

Oral presentation (45 min) performed on Feb. 10^{th} 2011 non-proportionality workshop.

Oral presentation (4 hrs) performed on March 7^{th} 2011 for the Schubert review.

Poster presentation at the Radsensing2011 meeting at the Sandia National Lab.

Invited presentation at Wake Forrest University on October 20, 2011.

Publication in Phys. Rev. B. : D. Aberg, B. Sadigh, P. Erhart, "Electronic structure of $LaBr_3$ from quasiparticle self-consistent GW calculations", Phys. Rev. B**85**, 125134 (2012).

Invited presentation at Non-proportionality workshop in PNNL in March 2012.

Contributed presentation at American Physical Society March Meeting 2012.

Invited paper: Qi Li, R.T. Williams, D. Aberg, "First-principles calculations and experiment predictions for iodine vacancy centers in SrI_2", Physica Status Solidi **250**, 233-243 (2013).

Contributed presentation at Sorma West 2012 in Oakland/CA

Invited presentation at Non-proportionality workshop in Oakland following Sorma2012 on 5-18-2012

Invited presentation at Radsensing2012 in Sandia/NM

Invited presentation at ICDIM2012 in Santa Fe/NM

Invited presentation at Radsensing2012 in Sandia/NM